Homeostatic control of the excitation-inhibition balance in cortical layer 5 pyramidal neurons.

Nicolas Le Roux, Muriel Amar, Gérard Baux, Philippe Fossier

HAL Id: hal-00147438

https://hal.science/hal-00147438

Submitted on 17 May 2007

Homeostatic control of the excitation–inhibition balance in cortical layer 5 pyramidal neurons

Nicolas Le Roux, Muriel Amar, Gérard Baux and Philippe Fossier
CNRS, Institut de Neurobiologie Alfred Fessard, FRC2118, Laboratoire de Neurobiologie Cellulaire et Moléculaire, UPR9040, Gif sur Yvette, F-91198, France

Abstract

Homeostatic regulation in the brain is thought to be achieved through a control of the synaptic strength by close interactions between excitation and inhibition in cortical circuits. We recorded in a layer 5 pyramidal neuron of rat cortex the composite response to an electrical stimulation of various layers (2–3, 4 or 6). Decomposition of the global conductance change in its excitatory and inhibitory components permits a direct measurement of excitation–inhibition (E-I) balance. Whatever the stimulated layer was, afferent inputs led to a conductance change consisting of 20% excitation and 80% inhibition. Changing synaptic strengths in cortical networks by using a high-frequency of stimulation (HFS) protocol or a low-frequency of stimulation (LFS) protocol (classically used to induce long-term potentiation or long-term depression at the synaptic level) were checked in order to disrupt this balance. Application of HFS protocols in layers 2–3, 4 or 6, or of LFS protocols in layer 4 induced, respectively, long-term paralleled increases or long-term paralleled decreases in E and I which did not change the E-I balance. LFS protocols in layers 2–3 or 6 decreased E but not I and disrupted the balance. It is proposed that regulatory mechanisms might be mainly sustained by recurrent connectivity between excitatory and inhibitory neuronal circuits and by modulation of shunting GABA$_A$ inhibition in the layer 5 pyramidal neuron.

Introduction

The neuronal population of the cerebral cortex is mainly composed of glutamatergic pyramidal neurons and gamma amino butyric acid (GABA)ergic interneurons making extensive local connections. Each cortical population also receives inputs from neighbouring neurons (Peters & Kara, 1985a; Martin, 2002) which form recurrent excitatory and inhibitory circuits. Moreover, excitatory circuits are strongly connected to inhibitory circuits (Maffei *et al*., 2004) of distinct types (Peters & Kara, 1985b; Gibson *et al*., 1999) by feedback and feedforward connections (Bannister, 2005).

The cortical response elaborated by layer 5 pyramidal neurons is dependent on the balance between the excitatory and inhibitory inputs perceived (Borg-Graham *et al*., 1998; Wehr & Zador, 2003). Thus, the regulation of cortical activity needs a tight control of excitatory and inhibitory neurons; a complex control of the excitation–inhibition (E-I) balance has to be maintained to keep the network in a functional state (Liu, 2004; Haider *et al*., 2006) to prevent saturation and hence disorders induced by hyper- or hypoexcitability (Turrigiano, 1999). In this way, neuronal networks can sense and control their level of excitability by adjusting their synaptic strength. This regulation has been described in terms of homeostatic plasticity (Davis & Bezprozvanny, 2001; Buckby *et al*., 2006). It is generally thought that dynamic equilibria between recurrent excitation and inhibition in neuronal networks allow the generation of stable periods of activity (Durstewitz *et al*., 2000; Compte *et al*., 2003; Turrigiano & Nelson, 2004). However, the only way to demonstrate experimentally that an equilibrated and regulated balance exists between excitation and inhibition is to determine the E-I ratio by a direct measurement of each component.

Our results provide experimental evidence for the previous computational analysis (Miller, 1996; Shu *et al*., 2003) predicting a homeostatic regulation of the E-I balance. In order to define the E-I balance in layer 5 pyramidal neurons, we used a method allowing simultaneous measurement of changes in excitation and inhibition conductances (Borg-Graham *et al*., 1998; Monier *et al*., 2003). Such a method used to determine the E-I balance at the somatic level of the pyramidal neuron permits maintenance of functional interactions between glutamatergic neurons and GABAergic interneurons because it avoids any pharmacological treatment of neuronal networks. Whichever network of the three main entries into the cortex (layers 2–3, 4 or 6) was stimulated, we observed that the E-I ratio was identical. To further investigate the regulatory mechanisms, we used protocols of stimulation known to induce changes in synaptic strength: a high-frequency stimulation (HFS) protocol classically used to induce long-term potentiation (LTP) and a low-frequency stimulation (LFS) protocol used to induce long-term depression (LTD) in the stimulated layer. Our results point to a network organization involving recurrent excitatory and inhibitory circuits which interact to stabilize the E-I balance and to assume neuronal control of synaptic integration. The control of the synaptic integration is partly due to tonic GABA$_A$ inhibition (known as shunting inhibition: Petrini *et al*., 2004; Mody, 2005) which appears differently recruited from one layer to another.

Materials and methods

Slice preparation

Parasagittal slices containing primary visual cortex were obtained from 18- to 25-day-old Wistar rats. Briefly, in accordance with the

guidelines of the American Neuroscience Association, a rat was decapitated, its brain quickly removed and placed in chilled (5 °C) artificial cerebrospinal extracellular solution. Slices of 250 μm thickness were made using a vibratome from the primary visual cortex and then incubated for at least 1 h at 36 °C in a solution containing (in mM): NaCl, 126; NaHCO$_3$, 26; glucose, 10; CaCl$_2$, 2; KCl, 1.5; MgSO$_4$, 1.5; and KH$_2$PO$_4$, 1.25 (pH 7.5, 310–330 mOsm). This solution was bubbled continuously with a mixture of 95% O$_2$ and 5% CO$_2$.

Electrophysiological recordings and cell identification

Slices were placed on the *X-Y* translation stage of a microscope with a video-enhanced differential interference contrast system and superfused continuously. The optical monitoring of the patched cell was achieved with standard optics using 40× long working distance water-immersion lens. Layer 5 pyramidal neurons, identified from the shape of their soma and primary dendrites and from their current-induced excitability pattern, were studied using the patch-clamp technique in whole-cell configuration. Somatic whole-cell recordings were performed at room temperature using borosilicate glass pipettes (of 3–5 MΩ resistance in the bath), filled with a solution containing (in mM): K-gluconate, 140; HEPES, 10; ATP, 4; MgCl$_2$, 2; GTP, 0.4; and EGTA, 0.5 (pH 7.3 adjusted with KOH, 270–290 mOsm).

Current-clamp and voltage-clamp recordings were performed using an Axopatch 1D (Axon Instruments, Union City, California, USA); filtered by a low-pass Bessel filter with a cutoff frequency set at 2 kHz, and digitally sampled at 4 kHz. The membrane potential was corrected off-line by −10 mV to account for the junction potential. This value (−10 mV) was measured in our experimental conditions (data not shown). Estimation of the access resistance (Rs) is critical in quantitatively evaluating the relative change in input conductance in response to synaptic activation. After capacitance neutralization, bridge balancing was performed on-line in current-clamp conditions, which provided us with an initial estimate of Rs. This value was checked and revised as necessary off-line by fitting the voltage response to a hyperpolarizing current pulse with the sum of two exponentials. Under voltage-clamp conditions, the holding potential was corrected off-line using this Rs value (see below). Only cells with a resting membrane potential more negative than −55 mV and recordings with Rs < 25 MΩ were kept for further analysis. In 350 cells, mean ± SD Rs = 18.4 ± 0.3 MΩ, ranging from 4 to 25 MΩ. The firing profile of neurons was determined in response to depolarizing current pulses ranging from −100 to +200 pA under current-clamp conditions.

The stimulating electrodes were positioned in the three main entrance sites of visual cortex: layers 4, 2–3 and 6. Electrical stimulations (1–10 μA, 0.2 ms duration) were delivered in these layers using 1 MΩ impedance bipolar tungsten electrodes (TST33A10KT; WPI, Hertfordshire, UK). The intensity of the stimulation was adjusted in current-clamp conditions to be strong enough to induce a subthreshold postsynaptic response due to coactivation of excitatory and inhibitory circuits but weak enough to avoid recruitment of dominant nonlinear processes linked for instance to NMDA receptor activation. Additional experiments (not shown) with the NMDA receptor blocker D-AP5 showed no variation in synaptic responses. Responses with antidromic spikes were discarded. Under voltage-clamp conditions, the frequency of stimulation was 0.05 Hz and five to eight trials were repeated for a given holding potential.

A control recording was made after 15 min of patch-clamp equilibration, and then HFS or LFS protocols were applied in order to induce long-term modifications of synaptic strengths in the recruited circuits. The HFS protocol was elicited with theta-burst stimulation, known to induce LTP at the synaptic level. It consisted of three trains of 13 bursts applied at a frequency of 5 Hz, each burst containing four pulses at 100 Hz (Abraham & Huggett, 1997). Several LFS protocols were tested (to induce LTD at the synaptic level): 1 Hz stimulation for 15 min (Dudek & Bear, 1992) or for 10 min, or 1 Hz stimulation for 10 min with bursts composed of eight pulses at 250 Hz. The first protocol gave better results and was retained. Recordings under control conditions were made at 0.05 Hz and an identical frequency of stimulation was used 15, 30, 45 and 60 min after application of the HFS or LFS protocol.

Synaptic response analysis

Data were analysed off-line with specialized software (Acquis1^{TM} and Elphy^{TM}; Biologic UNIC–CNRS, Gif-sur-Yvette, France). The method is based on the continuous measurement of conductance dynamics during stimulus-evoked synaptic response, as primary described *in vivo* on cat cortex (Borg-Graham *et al.*, 1998; Monier *et al.*, 2003). This method received further validation on rat primary auditory cortex (Wehr & Zador, 2003), on slices of ferret prefrontal and occipital cortex (Shu *et al.*, 2003; Haider *et al.*, 2006) and on rat barrel cortex (Higley & Contreras, 2006). Evoked synaptic currents were measured and averaged at a given holding potential. In *I-V* curves for every possible delay (t), the value of holding potential (Vh) was corrected (Vhc) from the ohmic drop due to the leakage current through Rs according the following equation.

$$V\mathrm{hc}(t) = V\mathrm{h}(t) - I(t) \times R\mathrm{s}$$

An average estimate of the input conductance waveform of the cell was calculated from the best linear fit (mean least square criterion) of the *I-V* curve for each delay (t) following the stimulation onset. Only cells showing a Pearson correlation coefficient > 0.95 for the *I-V* linear regression between −90 and −40 mV were considered when calculating the conductance change of the recorded pyramidal neuron from the slope of the linear regression.

The evoked synaptic conductance term [gT(t)] was derived from the input conductance by subtracting the resting conductance (g_{rest}). Under our experimental conditions, the global spontaneous activity was very weak and, thus, the synaptic activity at rest was null. Consequently, the g_{rest} value was estimated 90 ms before the electrical stimulation. The apparent reversal potential of the synaptic current at the soma [Esyn(t)] was taken as the voltage abscissa of the intersection point between the *I-V* curve obtained at a given time (t) and that determined at rest. Assuming that the evoked somatic conductance change reflects the composite synaptic input reaching the soma, Esyn(t) characterizes the stimulation-locked dynamics of the balance between excitation and inhibition.

Stable patch-clamp recordings were obtained from the soma of neurons, localized exclusively in layer 5 of rat visual cortex. The excitability profile of each neuron was characterized by the discharge pattern in response to test depolarizing current pulses. Recorded neurons had a resting potential of −75.7 ± 0.2 mV (n = 350) and showed the typical regular adaptation discharge pattern of pyramidal neurons. Membranes of these neurons had an input resistance of 240.0 ± 7.1 MΩ.

Decomposition of the synaptic conductance

To decompose the global evoked synaptic conductance [gT(t)] into excitatory and inhibitory components [gE(t) and gI(t)], we used the following simplifications:

$$I\mathrm{syn}(t) = g\mathrm{E}(t)(E\mathrm{syn}(t) - E\mathrm{exc}) + g\mathrm{I}(t)(E\mathrm{syn}(t) - E\mathrm{inh})$$

and

$$g\mathrm{T}(t) = g\mathrm{E}(t) + g\mathrm{I}(t)$$

where Isyn(t) is the global synaptic current, Esyn(t) is the apparent reversal potential at the soma (see the previous paragraph), gE(t) and gI(t) are excitatory and inhibitory conductances, respectively, and Eexc and Einh are the reversal potentials for excitation and inhibition currents. Values of these reversal potentials were equal to 0 mV for excitation (Eexc) and to −80 mV for inhibition (Einh; see Supplementary material, Appendix S1), lumping the combined effects of the activation of GABA$_A$ and GABA$_B$ receptors in a single inhibitory component potential (Anderson *et al.*, 2000; Borg-Graham, 2001; Monier *et al.*, 2003). These values for the reversal potentials are classically accepted (Wehr & Zador, 2003; Higley & Contreras, 2006). However, in additional experiments (data not shown) where we used a pharmacological bath application of excitatory synaptic transmission blockers (CNQX, D-AP5) associated with QX314 in the intracellular solution (to block the GABA$_B$ component), the apparent synaptic reversal potential of the peak conductance was found to be stabilized at −80 mV and the remaining synaptically evoked response component was abolished by addition of bicuculline, a selective antagonist of GABA$_A$ receptors. The value of −80 mV used in the decomposition method is thus the reversal potential corresponding to GABA$_A$ (and not an intermediate value between GABA$_A$ and GABA$_B$) because in the presence of QX314 no variation in the synaptic response was observed. Indeed, under our experimental conditions of stimulation of cortical layers leading to subthreshold postsynaptic responses, Esyn(t) which was extrapolated from *I-V* curves took any intermediate value between −80 and −40 mV, i.e. within the limits of our voltage excursion (−90 to −40 mV) corresponding to the linearity of *I-V* curves and between the respective values of Einh and Eexc in such a way that the mathematical conditions of the simplification used to calculate gI(t) and gE(t) were fulfilled (see Supplementary material, Appendix S1).

Like all somatic recordings, our recordings cannot make rigorous estimates of synaptic events in the distal dendrites, and the conductance estimates are ratios of the overall excitatory and inhibitory drive contained in the local network stimulated (Haider *et al.*, 2006). However, our measurements are relative changes in conductance magnitude which reflect the cumulative contributions of excitation and inhibition arriving at proximal portions of the neuron. These relative conductance changes at the somatic level define a narrow window over which input integration and spike output can occur (Higley & Contreras, 2006).

Two parameters were used to quantify the synaptic conductance changes: the peak value and the integral (int) over a time window of 200 ms. The contribution of each component was expressed by the ratio of its integral value (int$g$E or int$g$I) to that of global conductance change (int$g$T). The time elapsed from the beginning of the stimulation to the peak of conductance changes (TESP) was measured in order to avoid errors due to the overlapping of the stimulation artefact with the onset of synaptic responses. Stimulation artefacts were replaced off-line by equivalent basal line on the recordings.

Reconstitution of the membrane potential

The dynamics of the membrane potential (VrecT) was reconstituted from the experimentally derived excitatory and inhibitory conductance profiles, on the basis of the prediction given by the combination of the different synaptic activation sources:

$$\frac{dV_m(t)}{dt} = \frac{g_{rest} + g\mathrm{T}(t)}{\tau g_{rest}}\left(\frac{g_{rest}E_{rest} + g\mathrm{T}(t)E\mathrm{syn}(t)}{g_{rest} + g\mathrm{T}(t)} - V_m(t)\right)$$

where τ is the membrane time constant measured at rest by injecting a 50 pA hyperpolarizing current step and E_{rest} is the resting potential.

VrecI or VrecE are also derived from this equation assuming that the voltage drive is only due to inhibitory or excitatory conductance profiles, respectively.

As our method gives gE and gI at the somatic level (i.e. after dendritic integration), we do not have an estimation of shunting inhibition due to the activation of GABA$_A$ receptors (which opens chloride permeability) in conditions where the reversal potential of Cl$^-$ is close to the resting potential. The activation of these receptors does act as a shunt of distal inputs (Bai *et al.*, 2001; Kullmann *et al.*, 2005; Mody, 2005).

To estimate the shunting inhibition previously reported by theoretical studies as a tonic-like GABA$_A$ conductance (Mitchell & Silver, 2003; Mody, 2005), the following parameter, described as the M factor (Koch *et al.*, 1990) was calculated.

$$\mathrm{M} = (\mathrm{int}V\mathrm{recT} - \mathrm{int}V\mathrm{recI})/(\mathrm{int}V\mathrm{recE})$$

using the integrals of VrecT, VrecI and VrecE.

M reflects the reducing coefficient of excitation by shunting inhibition at the somatodendritic level when the membrane potential is near the resting potential.
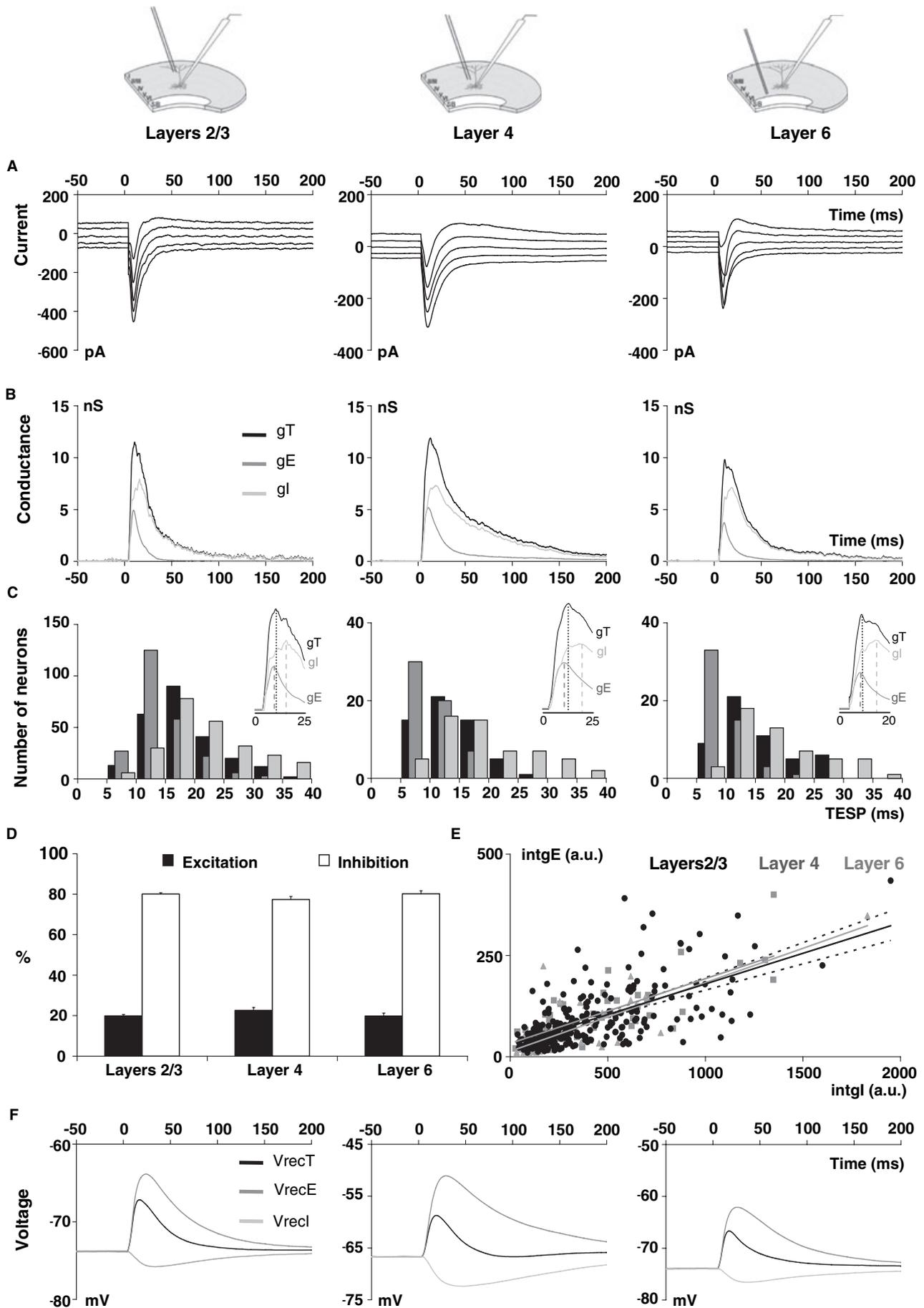
Statistical analysis

Data are expressed as the mean ± SD of n cells. Statistical analyses were performed using the nonparametric Wilcoxon test and the parametric t-test for paired samples. In this latter case, data were expressed as percentages of control values. Data were considered statistically significant for $P \leq 0.05$.

Results

Characterization of the E-I balance in layer 5 pyramidal neurons in response to the stimulation of different cortical layers

The visual cortex receives sensory inputs from the retina, mainly in layer 4 (Bannister, 2005; Silberberg *et al.*, 2005) but also in layers 2–3 and 6 (Thomson *et al.*, 2002; Sincich & Horton, 2005). Electrical stimulations of layers 2–3, 4 or 6 initiate a complex current response in the recorded pyramidal neuron of layer 5 (Fig. 1A). Representative experiments for stimulation of layers 2–3 (n = 241), 4 (n = 57) and 6 (n = 52) are presented in Fig. 1A. Figure 1B shows the decomposition of the conductance of the response (black trace) into its excitatory and inhibitory components (dark grey and light grey traces). The global conductance changes appeared with shorter TESP (black bars, Fig. 1C) when the stimulation was applied in layer 4 or 6 (15.0 ± 1.0 and 16.7 ± 1.2 ms, respectively) than in layers 2–3 (20.2 ± 0.6 ms). Similar results were obtained for excitatory (dark grey bars) or inhibitory (light grey bars) conductance changes. In all cases, excitation always occurred before inhibition. Stimulation in

© The Authors (2006). Journal Compilation © Federation of European Neuroscience Societies and Blackwell Publishing Ltd
European Journal of Neuroscience, **24**, 3507–3518

layer 4 or 6 induced excitation conductance changes with a preferential distribution between 5 and 10 ms after stimulation, and inhibition conductance changes between 10 and 15 ms. The excitation and inhibition conductance changes appeared later when the stimulation was applied in layers 2–3, i.e. between 10 and 15 ms and between 15 and 20 ms, respectively. It is proposed that excitatory afferents are directly recruited by the stimulation whereas inhibitory afferents (91.3% ± 4.8%, $n = 6$) depend on disynaptic connections involving a glutamatergic excitatory synapse on the GABAergic neuron (unpublished results obtained following excitation blockade) which introduce a delay for the observed inhibition in pyramidal neurons. The shorter TESP of the response induced by stimulation of layer 4 or 6 may result from the proximity of the soma of the pyramidal cell in layer 5 and/or from the neuronal composition and organization of the activated networks.

The integral of conductance changes was calculated as it reflects the conductance as a function of time with a better reproducibility than the direct measurement of the peak conductance. The analysis of the whole population of recorded neurons gave mean values of total conductance integral (intgT), 503.9 ± 23.1, 520.9 ± 51.5 and 319.9 ± 47.1 arbitrary units for stimulation of layers 2–3, 4 and 6, respectively. Similarly, changes in excitation (intgE) and inhibition (intgI) conductance integrals were calculated and expressed as percentages of intgT. Excitation represented ∼ 20% and inhibition 80% of the signal received by layer 5 pyramidal neurons, whichever layer was stimulated (Fig. 1D). The balance between excitatory and inhibitory inputs was also estimated by the slope of the linear regression of the relationships between intgE and intgI (Fig. 1E). Linear regressions corresponding to stimulation in layer 4 or 6 lie within the 95% confidence interval calculated for stimulation in layers 2–3. This confirms that E-I ratios were similar whichever layer of the cortical network was stimulated and although different neuronal networks were recruited. The large proportion of inhibition and the lack of change in this parameter through stimulation of different layers are in agreement with previous studies showing that inhibition appears to be the main controller of excitability in the cortex (Galarreta & Hestrin, 1998; Hasenstaub et al., 2005) although glutamatergic pyramidal cells represent > 80% of the neuronal population in each layer (Peters & Kara, 1985a). This is all the more crucial as GABAergic neurons are highly connected by electrical synapses (Bennett, 1997; Hestrin & Galarreta, 2005) which probably synchronize all recurrent GABAergic circuitry in the cortex (Buzsáki & Chrobak, 1995).

Reconstituted voltage responses of a pyramidal neuron, as well as the reconstituted voltage drives of excitation and inhibition during the response, following activation of different layers are shown in Fig. 1F. These subliminar responses to stimulation of one layer just reflect the result of somatodendritic integration of afferent inputs in the soma of the pyramidal neuron, i.e. the probability of occurrence of action potentials.

The voltage response is not the linear summation of reconstituted independent excitation and inhibition voltage changes due to shunting inhibition estimated by the M factor (see Materials and methods). M factor values were similar for stimulation of layers 2–3 and 4 (0.64 ± 0.01 and 0.65 ± 0.02, respectively) but lower than that for layer 6 stimulation (0.75 ± 0.02). These values emphasize that tonic-like GABA$_A$ inhibition acts as a somatodendritic filter for distal signals afferent to the pyramidal neuron, this filter being more or less important according to the stimulated layer. To approach the factors controlling the E-I balance, we next tried to modify the balance of excitatory and inhibitory inputs on the layer 5 pyramidal neuron by application of HFS or LFS protocols.

Effects of HFS or LFS protocols of stimulation in different cortical layers on the E-I balance

HFS and LFS are known to induce prolonged modifications of synaptic efficacy (LTP or LTD). They have been mainly studied on excitatory glutamatergic synapses in the hippocampus (Bliss & Gardner-Medwin, 1973), in the cortex (Daw et al., 2004) and in the cerebellum (Daniel et al., 1998). Few observations of LTP at inhibitory synapses have been made (Komatsu, 1996; Saitow et al., 2005). However, the consequences of HFS and LFS protocols of stimulation applied on a complex neuronal network have not been determined. In order to induce prolonged changes in synaptic efficacy in cortical networks, HFS or LFS protocols were applied in different cortical layers and the E-I balance was then determined in the layer 5 pyramidal neuron.

HFS protocols in layers 2–3 ($n = 12$), 4 ($n = 23$) or 6 ($n = 19$) led to an increase in current amplitudes of the recorded layer 5 pyramidal neuron (Fig. 2A). Marked increase in integrals of global, excitation and inhibition conductance changes compared to control were observed (Fig. 2B). These effects were recorded 15 min after HFS and were well maintained during a further 45 min. It is probable that they were due to long-term significant increases in synaptic efficacies. It is worth noting that intgT, intgE and intgI increased in the same proportions for stimulation of layers 2–3 or 6 by ∼ 50, 30 and 50%, respectively (see Fig. 2, B1, B2 and B3), whereas the effects were weaker for layer 4 (by ∼ 40, 20 and 40%, respectively; Fig. 2, B2) than for the other stimulated layers. However, no significant modification of the ratio of excitation or inhibition to total conductance changes was detected (Fig. 2C). This strongly suggests that equivalent enhancements of excitatory and inhibitory inputs occur after application of HFS to maintain the network in a stable functional range. Indeed, reconstituted voltage responses showed no significant variation in the response of the studied pyramidal neuron after HFS protocols in both excitatory and inhibitory input circuits, as illustrated in Fig. 2D for application of HFS in layers 2–3. However, the M factor was decreased after HFS protocols in layers 2–3 (from a control value of 0.61 ± 0.04 to 0.57 ± 0.04 after 60 min) or in layer 6 (from a

FIG. 1. Comparison of the effects of stimulation of different layers of rat visual cortex on the response recorded in layer 5 pyramidal neurons. Diagrams show the location of the stimulated layer (bipolar electrode, left) and of the recorded neuron ($n = 241$ for layers 2–3, $n = 57$ for layer 4 and $n = 52$ for layer 6) in layer 5 (micropipette, right). (A) Representative current recordings in response to electrical stimulation (100 ms) applied in the given layer. Holding potentials were scaled from −75 mV (bottom trace) to −55 mV (top trace) for layers 2–3; from −65 to −45 mV for layer 4; and from −70 to −50 mV for layer 6; a11 in 5-mV steps. (B) Decomposition of the total conductance change in the response (black) into its excitatory (dark grey) and inhibitory (light grey) components. Peak values of the total conductance changes were 11.7 ± 1.2, 11.6 ± 0.6 and 9.7 ± 1.5 nS for stimulations applied in layers 2–3, 4 and 6, respectively. (C) Distribution of TESP of the responses for the studied population of recorded pyramidal neurons. TESP values were calculated from time 0, the beginning of the stimulation, to the peak of the conductance changes: global (black), excitatory (dark grey) and inhibitory (light grey). Insets are the conductance changes presented in B on an expanded time scale. (D) Excitatory (black bars) and inhibitory (white bars) conductances expressed as percentages of the total conductance change. Note that excitation represents 19.9 ± 0.6%, 22.7 ± 1.4% and 19.9 ± 1.4% of total conductance change for stimulation of layers 2–3, 4 and 6, respectively. (E) Relationship between intgE and intgI for each recorded neuron. Linear regression (black line) with its 95% confidence interval (dotted lines) corresponds to layers 2–3 stimulation and has a slope of 0.1511. The slopes of linear regressions for stimulations of layers 4 (dark grey line) or 6 (light grey line) were 0.1599 and 0.1695, respectively. (F) Reconstitution of the voltage responses from membrane parameters: global voltage drive (black line); voltage drive considering the sole contribution of excitation (dark grey line); and voltage drive considering the sole contribution of inhibition (light grey line).
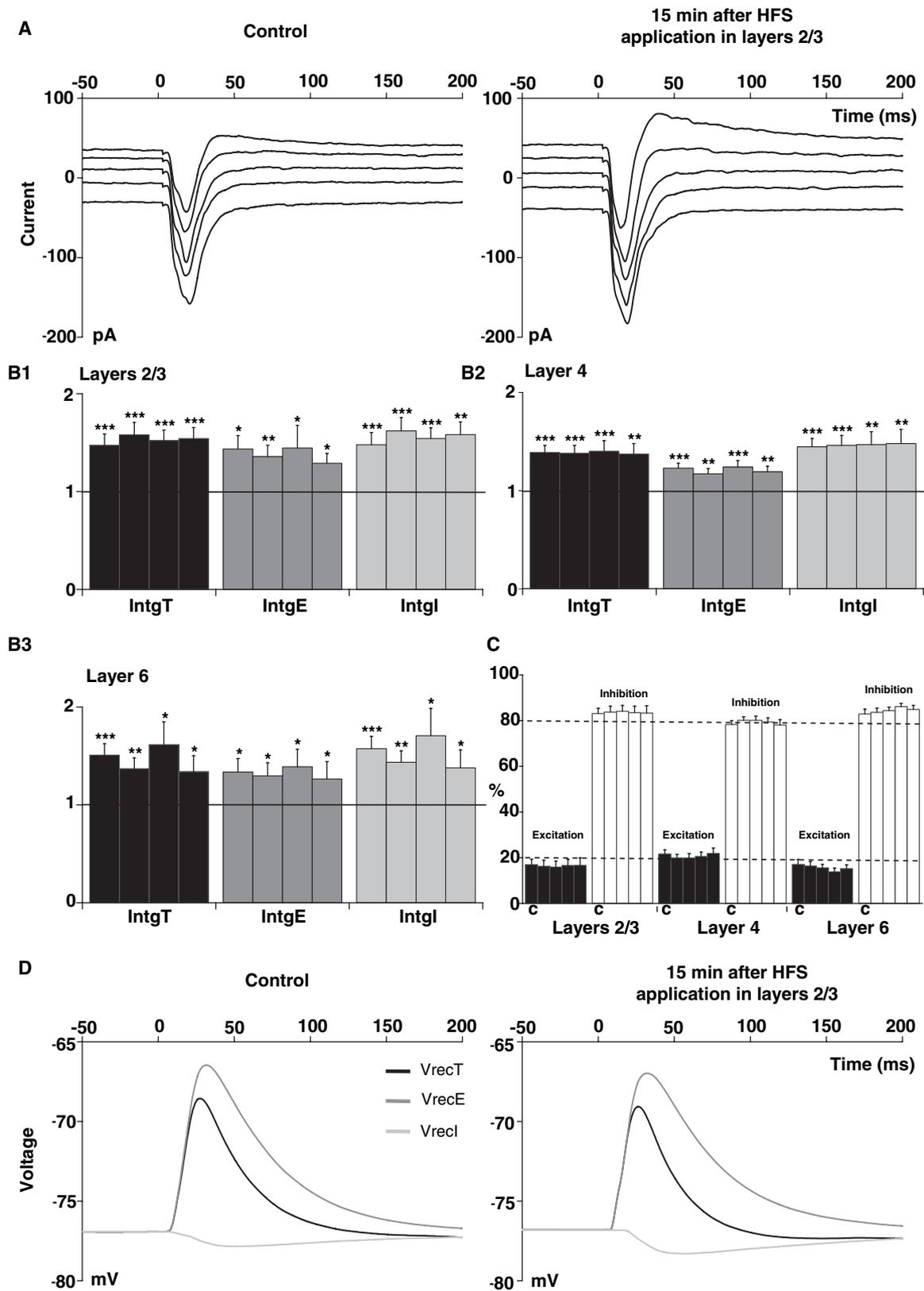
FIG. 2. Effects of HFS protocols. (A) Representative whole-cell current recordings before and 15 min after application of HFS in layers 2–3. Holding potentials were scaled from −85 mV (bottom trace) to −65 mV (top trace), in 5-mV steps. (B) Relative changes (compared to control) of intgT (black bars), intgE (dark grey bars) and intgI (light grey bars), various times (15, 30, 45 and 60 min) after application of HFS in layers 2–3 ($n = 12$), 4 ($n = 23$) and 6 ($n = 19$). (C) Relative contribution of excitation (black) and inhibition (white) conductances to the total conductance change, various times (15, 30, 45 and 60 min) after HFS protocols in the different layers (c, control). (D) Reconstitution of the voltage responses from membrane parameters. Global voltage drive (black line), voltage drive considering the sole contribution of excitation (dark grey line), and voltage drive considering the sole contribution of inhibition (light grey line) before and 15 min after application of HFS in layers 2–3. Note that the voltage drive was unchanged after the HFS protocol. ***$P < 0.001$, **$P < 0.01$, *$P < 0.05$.
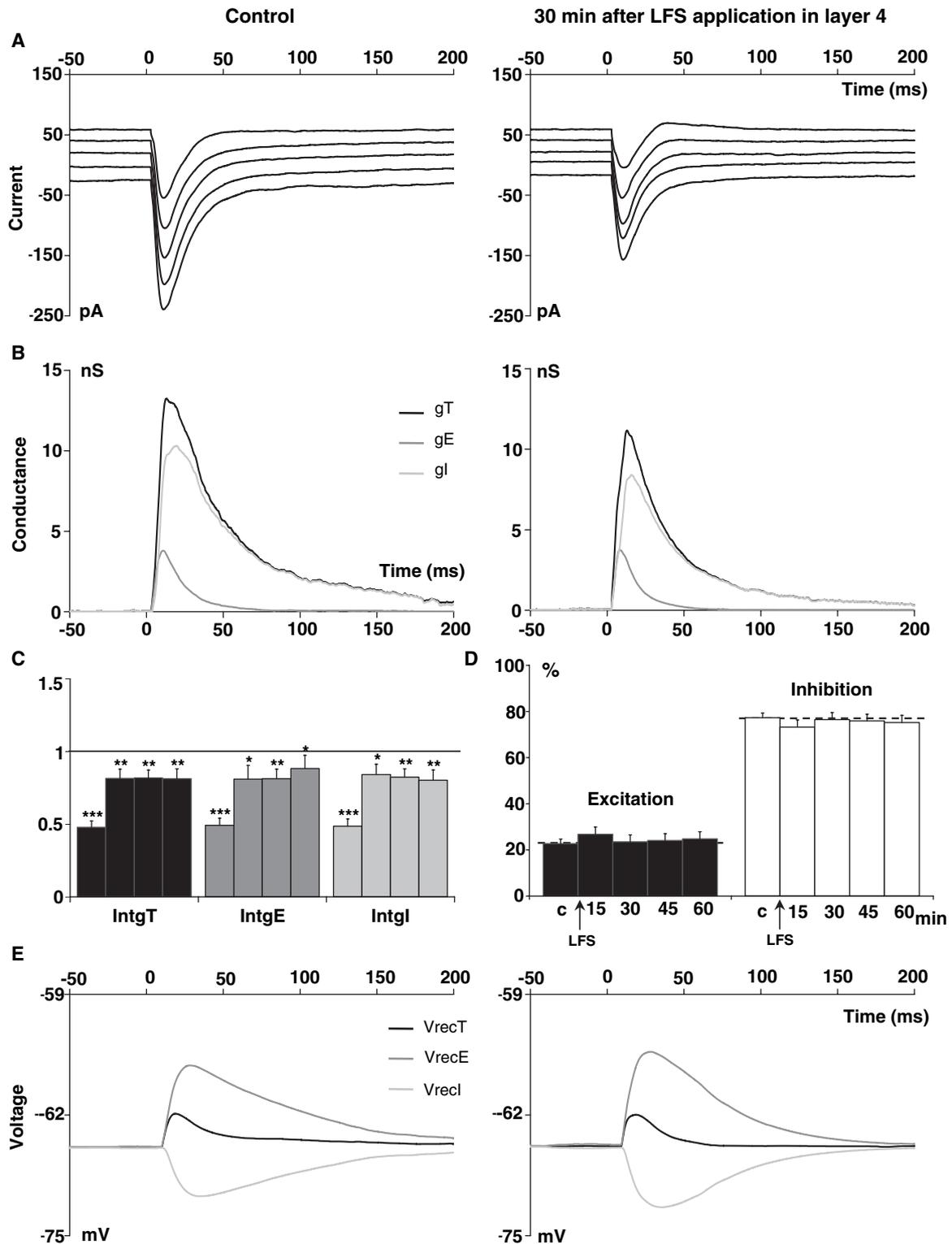
FIG. 3. Effects of LFS protocols in layer 4. (A) Representative whole-cell current recordings before and 30 min after application of LFS in layer 4. Holding potentials were scaled from −85 mV (bottom trace) to −65 mV (top trace), in 5-mV steps. (B) Decomposition of the total conductance change in the response (black) into its excitatory (dark grey) and inhibitory (light grey) components before and after the LFS protocol. (C) Relative changes (compared to control) of intgT (black bars), intgE (dark grey bars) and intgI (light grey bars), various times (15, 30, 45 and 60 min) after application of LFS ($n = 23$). The excitatory conductance was decreased by $18 \pm 6\%$ and the inhibitory conductance by $17 \pm 5\%$. (D) Relative contribution of excitation (black) and inhibition (white) conductances to the total conductance change, various times (15, 30, 45 and 60 min) after the LFS protocol in layer 4 (c, control). (E) Reconstitution of the voltage responses from membrane parameters before and after LFS protocols: global voltage drive (black line), voltage drive considering the sole contribution of excitation (dark grey line), and voltage drive considering the sole contribution of inhibition (light grey line). Note that the voltage drive was unchanged after LFS. ***$P < 0.001$, **$P < 0.01$, *$P < 0.05$.

control value of 0.72 ± 0.03 to 0.62 ± 0.04 after 60 min) but was unchanged after HFS in layer 4 (0.69 ± 0.04). These significant ($P < 0.05$) decreases in the M factor indicate an increase in the shunting inhibition. This may be due to an enhancement of shunting GABA$_A$ inhibition at a somatodendritic level after HFS protocols in layers 2–3 or 6. In contrast, HFS protocols in layer 4 did not seem to have a marked effect on tonic GABA$_A$ inhibition. We conclude that, according to the stimulated layer, potentiating effects of the excitatory inputs due to HFS is significantly balanced by the potentiation of hyperpolarizing inhibitory inputs and/or by shunting inhibition.

In order to induce synaptic depressions in stimulated neuronal circuits, a 15 min stimulation at 1 Hz (LFS protocol) in layers 2–3 ($n = 17$), 4 ($n = 23$) or 6 ($n = 22$) was used. Representative results of LFS in layer 4 are shown in Fig. 3. They involved a decrease in both current amplitudes (Fig. 3A) and conductance changes (Fig. 3B). The large decrease (by 50%) of the conductance following 15 min recordings was not considered for analysing the results because it corresponds to the end of the stimulation. The integral of excitatory conductance was significantly decreased, by $18 \pm 6\%$, and the integral of inhibitory conductance by $17 \pm 5\%$; these effects were sustained following LFS protocols (Fig. 3C). However, the integrals of excitation and inhibition conductance changes, expressed as percentages of that of global conductance change, were not significantly modified (Fig. 3D). This indicates that the E-I ratio was not affected by LFS in layer 4. Reconstituted voltage recordings for layer 4 stimulation revealed no significant modification in the responses after LFS protocols (Fig. 3E). However, the M factor was increased (from 0.66 ± 0.04 for control to 0.71 ± 0.03 after 60 min). This significant ($P < 0.01$) increase indicates a lower effect of shunting inhibition than under control conditions.

Interestingly, LFS of layers 2–3 or 6 induced a significant decrease in the integral of excitation conductance change whereas that corresponding to inhibition was slightly enhanced (Fig. 4A). Significant ($P < 0.05$) decreases in the ratio of excitation to total conductance changes were observed for stimulation of layers 2–3 (by $24 \pm 9\%$) and for stimulation of layer 6 (by $22 \pm 8\%$), as expected with the LFS protocol. However, inhibition was significantly ($P < 0.05$) increased, by 8 ± 2 and $7 \pm 2\%$, respectively (Fig. 4B). These unexpected results indicate a decrease in the E-I ratio which was further confirmed by the statistical analysis of linear regressions of the relationships between intgE and intgI. It is worth noting that after various times (30–60 min) following LFS in layer 4, linear regressions were well fitted in the 95% confidence interval of the control, indicating no effect on the E-I ratio (Fig. 4, C1). In contrast, linear regressions did not lie within the 95% confidence interval of the control after LFS in layers 2–3 (Fig. 4, C2) or in layer 6 (Fig. 4, C3). These modifications of the E-I ratio led to a marked decrease in the depolarizing phase of the reconstituted voltage response, as illustrated

in Fig. 4D and E. In this case, the M factor was not significantly modified after the LFS protocol in layer 6 (0.78 ± 0.03 for control and 0.77 ± 0.03 after 60 min) and a similar observation was made for LFS protocols in layers 2–3. This indicates that application of LFS in layers 2–3 or 6 modified the ratio between excitation and hyperpolarizing inhibition without significantly changing shunting GABA$_A$ inhibition in the layer 5 pyramidal neuron.

We conclude that changes in the E-I balance appear to be linked to the specific organization of various cortical layers (see Xiang *et al.*, 2002) to involve feedback and feedforward connections between pyramidal neurons and inhibitory interneurons. The opposite effects observed on the shunting inhibition when layers 2–3 or 6 and layer 4 were stimulated are in favour of a particular mode of activation of shunting GABA$_A$ inhibition which clearly appears to be at least frequency-dependent.
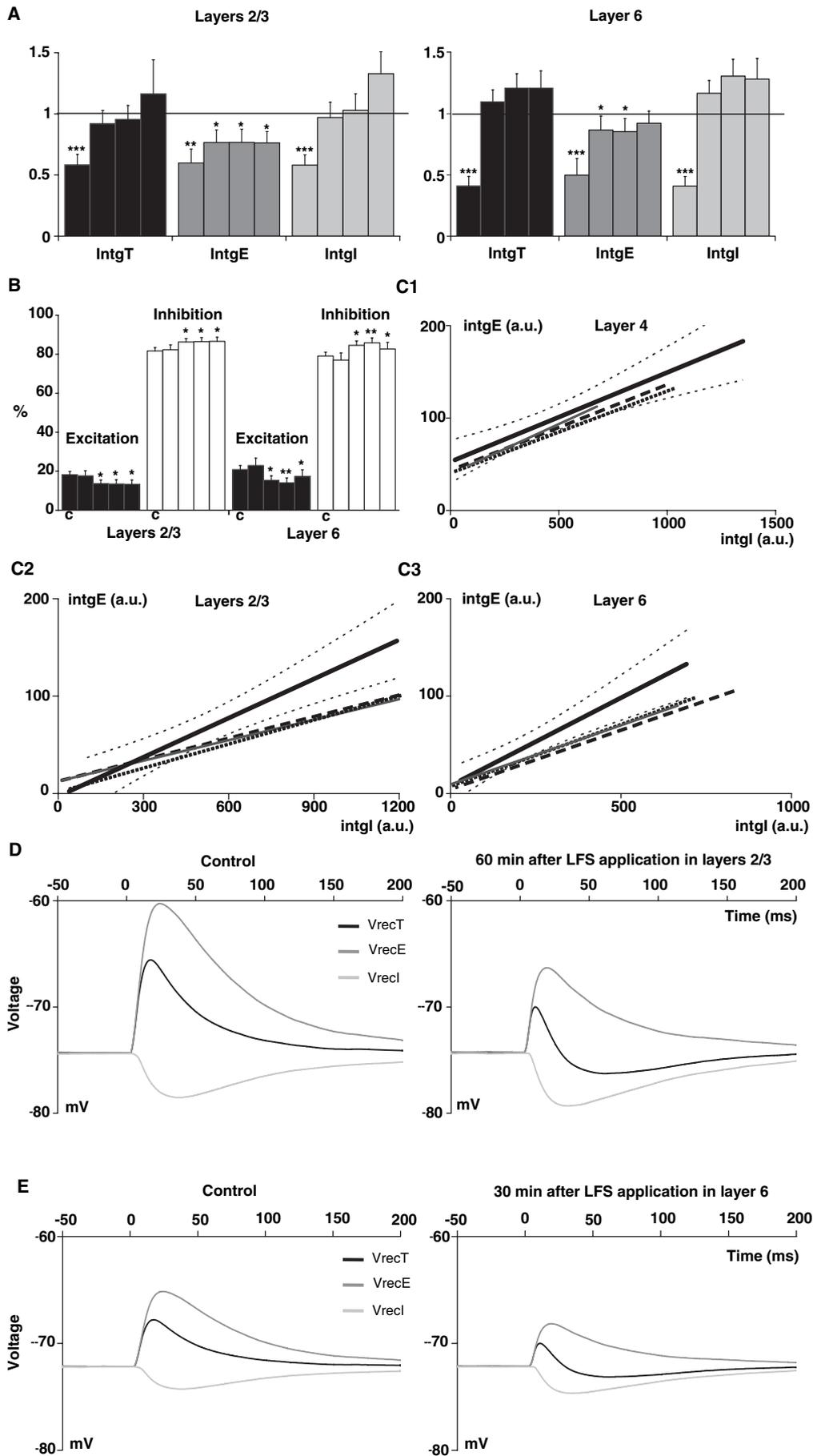
Discussion

A homeostatic regulation of the E-I balance has been proposed as preserving the structure and the function of neuronal networks (Maffei *et al.*, 2004). Our study clearly shows that, in cortical networks, the E-I balance measured at the somatic level of a pyramidal neuron of layer 5 is not dependent on the stimulated layer, and is characterized by an excitatory component accounting for 20% of the global conductance change and by an inhibitory component accounting for 80%. This balance is not markedly modified by protocols of stimulation that change the synaptic strength (such as HFS whichever layer was stimulated or LFS protocols in layer 4). It can be also disrupted by some protocols (as we have seen for application of LFS in layers 2–3 or 6).

Estimation of the relative contributions of excitation and inhibition to the global conductance change is based on a method of conductance calculation in which it is assumed that neurons are linear isopotential neurons. According to Wehr & Zador (2003), the deviation of the actual membrane from these assumptions results in an underestimate of conductance magnitudes that is greater for inhibitory than excitatory inputs. Saturation and synaptic current attenuation also reduce the effective excitatory and inhibitory conductances seen from the soma. Indeed, these factors do not represent solely errors of estimation but reflect functional consequences of somatodendritic integration (Wehr & Zador, 2003). It is precisely the result of integration which appeared in the reconstituted voltage response in our work.

Comparing effects of the stimulation of different layers on the response recorded in layer 5 pyramidal neurons shows the following. (i) Whichever layer is stimulated, excitation occurs before inhibition but the TESP of the response is shorter for layer 4 or 6 stimulation

---

Fig. 4. Effects of LFS protocols in layers 2–3 or 6. (A) Relative changes (compared to control) of intgT (black bars), intgE (dark grey bars) and intgI (light grey bars), various times (15, 30, 45 and 60 min) after application of LFS in layers 2–3 ($n = 17$) or in layer 6 ($n = 22$). (B) Relative contribution of excitation (black) and inhibition (white) conductances to the total conductance change, various times after LFS protocols in layers 2–3 or 6 (c, control). (C) Relationships between intgE and intgI. (C1) The linear regression (thick black line) and its 95% confidence interval is represented for the control condition (slope of regression was 0.0964). Slope of linear regressions 30 min (thin black line), 45 min (dashed line) and 60 min (dotted line) after application of the LFS protocol in layer 4 were 0.1082, 0.0923 and 0.0893, respectively. Note that these linear regressions lie within the 95% confidence interval of the control. (C2) Linear regressions of intgE as a function of intgI for control conditions (thick black line, slope = 0.2025) with its 95% confidence interval, and 30 min (thin black line, slope = 0.1809), 45 min (dashed line, slope = 0.1782) and 60 min (dotted line, slope = 0.1871) after stimulation with the LFS protocol in layers 2–3. (C3) Linear regressions of intgE as a function of intgI for control conditions (thick black line, slope = 0.1793) with its 95% confidence interval, and 30 min (thin black line, slope = 0.1244), 45 min (dashed line, slope = 0.1197) and 60 min (thick black line, slope = 0.1268) after stimulation with the LFS protocol in layer 6. Note (C2 and C3) that linear regressions do not lie within the 95% confidence interval of the control following LFS protocols in layers 2–3 or 6. (D) Reconstitution of the voltage responses from membrane parameters before and after an LFS protocol applied to layers 2–3: global voltage drive (black line), voltage drive considering the sole contribution of excitation (dark grey line), and voltage drive considering the sole contribution of inhibition (light grey line). Note that a marked decrease in the depolarizing phase of the response was observed after the LFS protocol. (E) Reconstitution of the voltage responses from membrane parameters before and after the LFS protocol in layer 6 (identical meaning of shades of grey as in D). Note that a marked decrease in the depolarizing phase of the response was observed after the LFS protocol.

than for layers 2–3 stimulation. Although this observation might be linked to the distance of the stimulating electrode (more or less distant from the recorded pyramidal neuron), it also indicates some difference in the composition of stimulated networks. (ii) Shunting inhibition evoked by stimulation of layers 2–3 or 4 is identical. This may be due to the recruitment of GABA receptors localized on the apical dendrite (Xiang *et al.*, 2002; Monier *et al.*, 2003) of the recorded neuron because it has been proposed that these receptors are responsible for shunting inhibition (Staley & Mody, 1992) whereas stimulation of layer 6 recruits mainly GABA receptors on the soma. (iii) The results obtained after application of HFS or LFS protocols in layer 4 were different from those obtained by stimulations of layers 2–3 or 6. HFS protocols induced a weaker potentiation of the inputs for layer 4 stimulation than for stimulation of layers 2–3 or 6, whereas LFS protocol application disrupted the E-I balance for stimulation of layers 2–3 or 6, in contrast to layer 4.

These observations support an activation of different networks which can differ in their composition of excitatory and inhibitory neurons and their properties of signal modulation (Gibson *et al.*, 1999) although we cannot rule out upstream modulations by other neuro-modulators, depending on the location of stimulating electrodes. However, it is surprising that the stimulation of different layers induces responses in the layer 5 pyramidal neurons which are characterized with our experimental procedure by a large proportion (80%) of inhibitory inputs, although the majority of cortical neurons are excitatory neurons (Peters & Kara, 1985a; Somogyi *et al.*, 1998). Indeed, the cortical organization of excitatory and inhibitory neurons in networks creates specialized subpopulations of neurons (Yoshimura & Callaway, 2005). We have seen that excitation is always first recruited. This is physiologically achieved by inputs from the thalamus or from the cortex itself which activate excitatory networks leading to a secondary activation of inhibitory networks (Maffei *et al.*, 2004). Our results clearly show a main controlling function of inhibitory inputs on the probability of evoked action potential occurrence in the layer 5 pyramidal neurons. Inhibitory neurons compose a heterogeneous population of neurons with 12 described types (Gupta *et al.*, 2000) exhibiting various morphologies and functional properties (Cherubini & Conti, 2001), contrary to the excitatory pyramidal neurons which appear to form a homogeneous cell population. Studies in the neocortex have supported the idea that these different inhibitory networks could partly result from the electrical coupling (Hestrin & Galarreta, 2005) between similar types of local-circuit interneurons (Galarreta & Hestrin, 1999; Beierlein *et al.*, 2000) via gap junctions to the exclusion of other types of inhibitory neuron (Gibson *et al.*, 1999). The difference in the diversity of inhibitory populations recruited as a function of the stimulated layers in the cortex might explain the relative role of shunting inhibition in our experiments. Using recordings of layer 5 pyramidal neurons, it has been shown that low-threshold spike (LTS) interneurons of rat visual cortex layer 5 have numerous synapses on the apical dendrite which render them responsible for a strong shunting inhibition (Tamás *et al.*, 2000; Xiang *et al.*, 2002). Fast-spiking (FS) interneurons contact mainly the soma and the proximal dendrites of layer 5 pyramidal neurons to directly modulate the excitability through hyperpolarization or shunting inhibition but to a lesser extent than LTS neurons (Xiang *et al.*, 2002). These data are in accordance with our experiments showing that shunting inhibition is more efficient when the stimulation is applied in layers 2–3 (which can recruit the majority of LTS interneurons) compared to layer 6 stimulation (which can recruit FS interneurons). Despite this hetero-geneity in cortical networks, we observed an outstanding stability of the E-I ratio whichever the stimulated layer (2–3, 4 or 6) was.

Synaptic plasticity not only is a mechanism inducing learning and memory but also plays an important role in information processing and the control of excitability (Destexhe & Marder, 2004). In our study, application of HFS protocols was associated with a potentiation of excitatory inputs and a direct or an indirect potentiation of inhibition whichever layer was stimulated. Numerous studies have been carried out on long-term facilitation of glutamatergic transmission (Daw *et al.*, 2004) but much less is known about the gain control mechanisms and the plasticity of GABAergic transmission at inhibitory synapses. Indeed, a few studies report a direct potentiation of inhibitory synapses (Komatsu, 1996; Saitow *et al.*, 2005), but it seems more probable that an indirect disynaptic potentiation can occur in our system because it has been observed that, in layers 2–3, disynaptic activation (via a glutamatergic synapse) of inhibitory interneurons represents 90% of inhibition. HFS protocols enhance excitatory and inhibitory inputs on the layer 5 pyramidal neuron. It is obvious that we cannot localize facilitated synapses in the stimulated networks by HFS protocols, but what is important is the absence of significant variation in the E-I ratio otherwise illustrated by no change in the reconstituted voltage drive. A similar result was obtained for the LFS protocol applied in layer 4 with a depression of excitatory and inhibitory inputs but no change in the voltage drive of the response. Paralleled changes in excitatory and inhibitory inputs on the layer 5 pyramidal neuron avoid a significant modification of the E-I balance although these changes are probably due to remodelling of excitatory and inhibitory circuits after application of HFS or LFS protocols. One site of remodelling might be a change in the clustering of $GABA_A$ receptors leading to a modulation of shunting inhibition (Petrini *et al.*, 2004). Another possibility would be that gap junctions between GABAergic interneurons would be differently regulated by activity-dependent processes. Remodelling of the circuits may involve feedback projections of layer 5 pyramidal neurons on inhibitory circuits and feedforward connections with other pyramidal neurons (Bannister, 2005; Silberberg *et al.*, 2005).

The sensitivity of excitatory and inhibitory synapses to different frequencies of stimulation appears to be critical. Moreover, the heterogeneity of inhibitory interneurons in the cerebral cortex suggests that each type of cell has different biophysical properties (Gupta *et al.*, 2000; Markram *et al.*, 2004) as illustrated by FS interneurons which discharge strongly in relation to higher frequency stimulation (Hasenstaub *et al.*, 2005). In the cerebral cortex, the frequency of neuronal discharges peaks at 20 and 60 Hz; these frequencies characterize β and γ rhythms, respectively (Wespatat *et al.*, 2004). However, each neuronal type may have its own pattern of discharge as observed for pyramidal cells firing at rates ranging from 5 to 20 Hz (Steriade *et al.*, 1978). The β and γ rhythms serve for attention, in short- as well as in long-term memory (Wespatat *et al.*, 2004), and frequencies < 15 Hz would be involved in memory consolidation (Crochet *et al.*, 2005). Although it has been proposed that a high level of discharge in the cortical network ensures better stability of connectivity within the cortical circuitry (Crochet *et al.*, 2005), high frequencies of discharge due to a misregulated balance of E-I (inhibition failure) may lead to epilepsy (Fritschy & Brünig, 2003). In consequence, the E-I balance must be strictly controlled in order to avoid unwanted racing out of the system but must allow some plasticity. We show that HFS protocols using high-frequency pulses (100 Hz) are able to induce potentiation of both excitatory and inhibitory inputs on layer 5 pyramidal neurons; nevertheless, a homeostatic regulation takes place to prevent change in the E-I ratio. In a range of stimulations < 15 Hz (a frequency used in our LFS protocol) a disruption of the homeostatic control of excitation and inhibition was observed, thus leading to a change in the excitability of

the pyramidal neuron (a marked decrease in the depolarizing phase of the response is observed).

Homeostatic regulation mainly involves dynamic adjustment of excitatory and inhibitory circuits (Rutherford *et al*., 1998; Kilman *et al*., 2002; Turrigiano & Nelson, 2004). A factor that controls the gain of the pyramidal neuron is its ability to sense and adapt its excitability level by feedback projections, allowing the selective recruitment of inhibitory inputs which ensure a graded activation of shunting GABA$_A$ inhibition.

We propose that the regulation of the E-I balance is sustained not only by the homeostatic plasticity process due to reciprocal interactions between excitatory and inhibitory circuits but also by modulation of dendritic integration properties of the pyramidal neuron; these properties are thus another major factor in keeping cortical networks within their functional range.

Supplementary material

The following supplementary material may be found on www. blackwell-synergy.com

Appendix. S1. Supplementary information about methods

Acknowledgements

Abbreviations

E-I, excitation–inhibition; GABA, gamma amino butyric acid; HFS, high-frequency stimulation; int$g$E, excitatory conductance integral; int$g$I, inhibitory conductance integral; int$g$T, total conductance integral; LFS, low-frequency stimulation; LTD, long-term depression; LTP, long-term potentiation; Rs, access resistance; TESP, time elapsed from the beginning of the stimulation to the peak.

References

Abraham, W.C. & Huggett, A. (1997) Induction and reversal of long-term potentiation by repeated high-frequency stimulation in rat hippocampal slices. *Hippocampus*, **7**, 137–145.

Anderson, J.S., Carandini, M. & Ferster, D. (2000) Orientation tuning of input conductance, excitation, and inhibition in cat primary visual cortex. *J. Neurophysiol.*, **84**, 909–926.

Bai, D., Zhu, G., Pennefather, P., Jackson, M.F., Macdonald, J.F. & Orser, B.A. (2001) Distinct functional and pharmacological properties of tonic and quantal inhibitory postsynaptic currents mediated by gamma-aminobutyric acid (A) receptors in hippocampal neurons. *Mol. Pharmacol.*, **59**, 814–824.

Bannister, A.P. (2005) Inter- and intra-laminar connections of pyramidal cells in the neocortex. *Neurosci. Res.*, **53**, 95–103.

Beierlein, M., Gibson, J.R. & Connors, B.W. (2000) A network of electrically coupled interneurons drives synchronized inhibition in neocortex. *Nat. Neurosci.*, **3**, 904–910.

Bennett, M.V. (1997) Gap junctions as electrical synapses. *J. Neurocytol.*, **26**, 349–366.

Bliss, T.V. & Gardner-Medwin, A.R. (1973) Long-lasting potentiation of synaptic transmission in the dentate area of the unanaestetized rabbit following stimulation of the perforant path. *J. Physiol. (Lond.)*, **232**, 357–374.

Borg-Graham, L.J. (2001) The computation of directional selectivity in the retina occurs presynaptic to the ganglion cell. *Nat. Neurosci.*, **4**, 176–183.

Borg-Graham, L.J., Monier, C. & Frégnac, Y. (1998) Visual input evokes transient and strong shunting inhibition in visual cortical neurons. *Nature*, **393**, 369–373.

Buckby, L.E., Jensen, T.P., Smith, P.J. & Empson, R.M. (2006) Network stability through homeostatic scaling of excitatory and inhibitory synapses following inactivity in CA3 of rat organotypic hippocampal slice cultures. *Mol. Cell. Neurosci.*, **31**, 805–816.

Buzsáki, G. & Chrobak, J.J. (1995) Temporal structure in spatially organized neuronal ensembles: a role for interneuronal networks. *Curr. Opin. Neurobiol.*, **5**, 504–510.

Cherubini, E. & Conti, F. (2001) Generating diversity at GABAergic synapses. *Trends Neurosci.*, **24**, 155–162.

Compte, A., Sanchez-Vives, M.V., McCormick, D.A. & Wang, X.J. (2003) Cellular and network mechanisms of slow oscillatory activity (< 1 Hz) in a cortical network model. *J. Neurophysiol.*, **89**, 2707–2725.

Crochet, S., Fuentealba, P., Cisse, Y., Timofeev, I. & Steriade, M. (2005) Synaptic plasticity in local cortical network in vivo and its modulation by the level of neuronal activity. *Cereb. Cortex*, **5**, 618–631.

Daniel, H., Levenes, C. & Crepel, F. (1998) Cellular mechanisms of cerebellar LTD. *Trends Neurosci.*, **21**, 401–407.

Davis, G.W. & Bezprozvanny, I. (2001) Maintaining the stability of neural function: a homeostatic hypothesis. *Annu. Rev. Physiol.*, **63**, 847–869.

Daw, N., Rao, Y., Wang, X.F., Fischer, O. & Yang, Y. (2004) LTP and LTD vary with layer in rodent visual cortex. *Vision Res.*, **44**, 3377–3380.

Destexhe, A. & Marder, E. (2004) Plasticity in single neuron and circuit computations. *Nature*, **431**, 789–795.

Dudek, S.M. & Bear, M.F. (1992) Homosynaptic long-term depression in area CA1 of hippocampus and effects of N-methyl-D-aspartate receptor blockade. *Proc. Natl Acad. Sci. USA*, **89**, 4363–4367.

Durstewitz, D., Seamans, J.K. & Sejnowski, T.J. (2000) Neurocomputational models of working memory. *Nat. Neurosci.*, **3**, 1184–1191.

Fritschy, J.M. & Brünig, I. (2003) Formation and plasticity of GABAergic synapses: physiological mechanisms and pathophysiological implications. *Pharmacol. Ther.*, **98**, 299–323.

Galarreta, M. & Hestrin, S. (1998) Frequency-dependent synaptic depression and the balance of excitation and inhibition in the neocortex. *Nat. Neurosci.*, **1**, 587–594.

Galarreta, M. & Hestrin, S.A. (1999) Network of fast-spiking cells in the neocortex connected by electrical synapses. *Nature*, **402**, 72–75.

Gibson, J.R., Beierlein, M. & Connors, B.W. (1999) Two networks of electrically coupled inhibitory neurons in neocortex. *Nature*, **402**, 75–79.

Gupta, A., Wang, Y. & Markram, H. (2000) Organizing principles for a diversity of GABAergic interneurons and synapses in the neocortex. *Science*, **287**, 273–278.

Haider, B., Duque, A., Hasenstaub, A.R. & McCormick, D.A. (2006) Neocortical network activity in vivo is generated through a dynamic balance of excitation and inhibition. *J. Neurosci.*, **17**, 4535–4545.

Hasenstaub, A., Shu, Y., Haider, B., Kraushaar, U., Duque, A. & McCormick, D.A. (2005) Inhibitory postsynaptic potentials carry synchronized frequency information in active cortical networks. *Neuron*, **47**, 423–435.

Hestrin, S. & Galarreta, M. (2005) Electrical synapses define networks of neocortical GABAergic neurons. *Trends Neurosci.*, **28**, 304–309.

Higley, M.J. & Contreras, D. (2006) Balanced excitation and inhibition determine spike timing during frequency adaptation. *J. Neurosci.*, **26**, 448–457.

Kilman, V., van Rossum, M.C.W. & Turrigiano, G.G. (2002) Activity deprivation reduces miniature IPSC amplitude by decreasing the number of postsynaptic GABA (A) receptors clustered at neocortical synapses. *J. Neurosci.*, **22**, 1328–1337.

Koch, C., Douglas, R. & Wehmeier, U. (1990) Visibility of synaptically induced conductances changes: theory and simulations of anatomically characterized cortical pyramidal cells. *J. Neurosci.*, **10**, 1728–1744.

Komatsu, Y. (1996) GABA$_B$ receptors, monoamine receptors, and postsynaptic inositol triphosphate-induced Ca^{2+} release are involved in the induction of long-term potentiation at visual cortical inhibitory synapses. *J. Neurosci.*, **16**, 6342–6352.

Kullmann, D.M., Ruiz, A., Rusakov, D.M., Scott, R., Semyanov, A. & Walker, M.C. (2005) Presynaptic, extrasynaptic and axonal GABAA receptors in the CNS: where and why? *Prog. Biophys. Mol. Biol.*, **87**, 33–46.

Liu, G. (2004) Local structural balance and functional interaction of excitatory and inhibitory synapses in hippocampal dendrites. *Nat. Neurosci.*, **7**, 373–379.

Maffei, A., Nelson, S.B. & Turrigiano, G.G. (2004) Selective configuration of layer 4 visual cortical circuitry by visual deprivation. *Nat. Neurosci.*, **7**, 1353–1359.

Markram, H., Toledo-Rodriguez, M., Wang, Y., Gupta, A., Silberberg, G. & Wu, C. (2004) Interneurons of the neocortical inhibitory system. *Nat. Rev. Neurosci.*, **5**, 793–807.

Martin, K.A. (2002) Microcircuits in visual cortex. *Curr. Opin. Neurobiol.*, **12**, 418–425.

Miller, K.D. (1996) Synaptic economics: competition and cooperation in synaptic plasticity. *Neuron*, **17**, 371–374.

Mitchell, S.J. & Silver, R.A. (2003) Shunting inhibition modulates neuronal gain during synaptic excitation. *Neuron*, **38**, 433–445.

Mody, I. (2005) Aspects of the homeostatic plasticity of GABA$_A$ receptor-mediated inhibition. *J. Physiol. (Lond.)*, **562**, 37–46.

Monier, C., Chavane, F., Baudot, P., Graham, L.J. & Frégnac, Y. (2003) Orientation and direction selectivity of synaptic inputs in visual cortical neurons: a diversity of combinations produces spike tuning. *Neuron*, **37**, 663–680.

Peters, A. & Kara, D.A. (1985a) The neuronal composition of area 17 of rat visual cortex. I. The pyramidal cells. *J. Comp. Neurol.*, **234**, 218–241.

Peters, A. & Kara, D.A. (1985b) The neuronal composition of area 17 of rat visual cortex. II. The nonpyramidal cells. *J. Comp. Neurol.*, **234**, 242–263.

Petrini, E.M., Marchionni, I., Zacchi, P., Sieghart, W. & Cherubini, E. (2004) Clustering of extrasynaptic GABA (A) receptors modulates tonic inhibition in cultured hippocampal neurons. *J. Biol. Chem.*, **279**, 45833–45843.

Rutherford, L.C., DeWan, A., Lauer, H.M. & Turrigiano, G.G. (1998) BDNF has opposite effects on the quantal amplitude of pyramidal neuron and interneuron excitatory synapses. *Neuron*, **21**, 521–530.

Saitow, F., Suzuki, H. & Konishi, S. (2005) Beta-Adrenoceptor-mediated long-term up-regulation of the release machinery at rat cerebellar GABAergic synapses. *J. Physiol. (Lond.)*, **565**, 487–502.

Shu, Y., Hasenstaub, A. & McCormick, D.A. (2003) Turning on and off recurrent balanced cortical activity. *Nature*, **423**, 288–293.

Silberberg, G., Grillner, S., LeBeau, F.E.N., Maex, R. & Markram, H. (2005) Synaptic pathways in neuronal microcircuits. *Trends Neurosci.*, **28**, 541–551.

Sincich, L.C. & Horton, J.C. (2005) The circuitry of V1 and V2: integration of color, form, and motion. *Annu. Rev. Neurosci.*, **28**, 303–328.

Somogyi, P., Tamás, G., Lujan, R. & Buhl, E.H. (1998) Salient features of synaptic organisation in the cerebral cortex. *Brain Res. Brain Res. Rev.*, **26**, 113–135.

Staley, K.J. & Mody, I. (1992) Shunting of excitatory input to dentate gyrus granule cells by a depolarizing GABAA receptor-mediated postsynaptic conductance. *J. Neurophysiol.*, **68**, 197–212.

Steriade, M., Oakson, G. & Kitsikis, A. (1978) Firing rates and patterns of output and nonoutput cells in cortical areas 5 and 7 of cat during the sleep-waking cycle. *Exp. Neurol.*, **60**, 443–468.

Tamás, G., Eberhard, H.B., Lörincz, A. & Somogyi, P. (2000) Proximally targeted GABAergic synapses and gap junctions synchronize cortical interneurons. *Nat. Neurosci.*, **3**, 366–371.

Thomson, A.M., West, D.C., Wang, Y. & Bannister, A.P. (2002) Synaptic connections and small circuits involving excitatory and inhibitory neurons in layers 2–5 of adult rat and cat neocortex: triple intracellular recordings and biocytin labelling in vitro. *Cereb. Cortex*, **12**, 936–953.

Turrigiano, G.G. (1999) Homeostatic plasticity in neuronal networks: the more things change, the more they stay the same. *Trends Neurosci.*, **22**, 221–227.

Turrigiano, G.G. & Nelson, S.B. (2004) Homeostatic plasticity in the developing nervous system. *Nat. Rev. Neurosci.*, **5**, 97–107.

Wehr, M. & Zador, A.M. (2003) Balanced inhibition underlies tuning and sharpens spike timing in auditory cortex. *Nature*, **426**, 442–446.

Wespatat, V., Tennigkeit, F. & Singer, W. (2004) Phase sensitivity of synaptic modifications in oscillating cells of rat visual cortex. *J. Neurosci.*, **24**, 9067–9075.

Xiang, Z., Huguenard, J.R. & Prince, D.A. (2002) Synaptic inhibition of pyramidal cells evoked by different interneuronal subtypes in layer V of rat visual cortex. *J. Neurophysiol.*, **2**, 740–750.

Yoshimura, Y. & Callaway, E.M. (2005) Fine-scale specificity of cortical networks depends on inhibitory cell type and connectivity. *Nat. Neurosci.*, **8**, 1552–1559.